VARIABLE-LENGTH VERSUS FIXED-LENGTH CODING: ON TRADEOFFS FOR SOFT-DECISION DECODING

Sai Han and Tim Fingscheidt

Institute for Communications Technology, Technische Universität Braunschweig
Schleinitzstr. 22, 38106 Braunschweig, Germany
{s.han,t.fingscheidt}@tu-bs.de

ABSTRACT

Variable-length codes (VLCs) are widely used in media transmission. Compared to fixed-length codes (FLCs), VLCs can represent the same message with a lower bit rate, thus having a better compression performance. But inevitably, VLCs are very sensitive to transmission errors. In this work, based on the trellis representation for VLCs and the BCJR algorithm, we present a variable-length soft-decision decoder utilizing bit-wise channel reliability information and achieving a better error robustness in contrast to hard-decision decoding. Given the application of VLCs in audio coding showing both source correlation and variable block lengths, a strong dependency of performance is observed for both. Therefore, we point out tradeoffs of (soft-decision) decoded FLCs and VLCs depending on quantization bit rate, source correlation, and block length. We find that VLCs over AWGN channels are only recommended for very low source correlation in combination with very short block lengths and soft-decision decoding.

***Index Terms*—** VLC, soft-decision decoding, block length, trellis representation, BCJR

1. INTRODUCTION

In digital communications, a robust source decoder is desired for adverse transmission conditions. Traditional hard-decision source decoding is often times still widely used in many receivers. In case of residual bit errors after channel decoding, an additional error concealment is required, for instance, GSM Enhanced Fullrate [1], AMR [2], and AMR-WB [3].

Several soft-decision *channel* decoding schemes have been proposed in [4, 5]. Their soft output in the form of log-likelihood ratios (LLRs) has been used in soft-decision *source* decoding approaches such as [6–11]. Later on, soft-decision speech and audio decoders have been proposed: G.726 ADPCM [12], A-law PCM and GSM Fullrate speech coding [13], high-quality PCM audio [14], and AMR-WB [15]. The aforementioned schemes are based on fixed-length codewords for the quantized source symbols.

In order to achieve better compression performance for transmission, indices of quantized source symbols can be mapped to a variable number of bits using variable-length codes (VLCs). While in error-free transmission, VLCs allow the decoder to identify the start and end bit positions of each codeword, this is not the case over error-prone channels. The effect of error propagation becomes a serious problem for a VLC decoder. Some research has already dealt with error robustness of VLC decoders using soft information. Some of the approaches are non-trellis-based [16], while some others use the Viterbi algorithm based on a graphical representation or a trellis representation [17–19]. Applying the BCJR algorithm [20], either a bit-level soft-in/soft-out VLC decoder [21, 22] based on the trellis representation from [23] or a symbol-level soft-in/soft-out VLC decoder [24] based on an intuitive trellis representation have been derived. However, the source symbol in [24] is only modeled as zeroth-order Markov process. Based on the work in [24] and applying a first-order Markov source model, the VLC soft-decision decoder proposed by Kliewer and Thobaben allows a higher robustness [25].

Due to the high compression rate, VLCs are widely used for image, video, and audio coding. A soft decoder with bit-level trellis representation for Huffman codes has been proposed for iterative decoding of JPEG-coded images [26]. Soft-decision decoding of VLCs has also been applied to H.264 and H.263+ Recommendations [27, 28]. Applying the method in [24], the scale factors of the MPEG-AAC determining the quantization step size are reconstructed by soft-decision decoding [29]. It is found that the number of scale factors, which is called *block length* in this paper, varies in each frame. However, only results for a block length of 100 have been shown in both [24, 25]. Therefore, it is interesting to study the influence of block length and quantization in VLC soft-decision decoding.

In this paper, assuming only the total number of bits and symbols in a block being known, we provide a variable-length soft-decision decoding framework inspired from [25]. We present new insights by performing two major simulations for 2 bit and 4 bit quantized Gaussian AR(1) source symbols, each with four different block lengths and two different source correlations. Moreover, we discuss performance tradeoffs of fixed-length [11, 13] and variable-length soft-decision decoding for these different conditions.

This paper is organized as follows: In Section 2, we describe the algorithm for variable-length soft-decision decoding which includes the trellis representation, the calculation of a posteriori probabilities (APPs), and source symbol estimation. Section 3 discusses the simulation results. Finally, some conclusions are drawn in Section 4.

2. SOFT-DECISION VLC DECODER

2.1. Overview

The block diagram of the transmission system is depicted in Fig. 1. The source symbols inside a block $\mathbf{u} = (u_1, u_2, \ldots, u_n, \ldots, u_B)$ are multiplexed and then quantized, with B being the block length and $n \in \{1, 2, \ldots, B\}$ being the symbol time index. Each quantized source symbol is represented by a corresponding M bit quantization codebook index $i \in \mathcal{I} = \{0, 1, \ldots, 2^M{-}1\}$, or by a quantizer bit combination $\mathbf{x}_n = \{0, 1\}^M$. Thereafter, the VLC encoder (e. g., a Huffman code) maps each fixed-length M bit combination $\mathbf{x}_n$ to a

978-1-4799-2893-4/14/$31.00 ©2014 IEEE

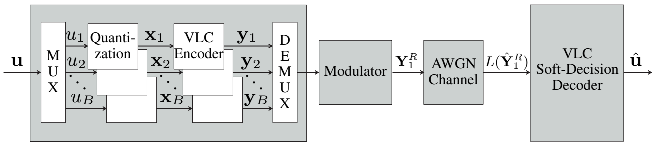

Fig. 1: Block diagram of the transmission system.

variable-length bit combination $\mathbf{y}_n \in \{0,1\}^{N^{(i)}}$, with $N^{(i)}$ being the codeword length of quantization codebook index i. After demultiplexing, a binary phase-shift keying (BPSK) modulator transforms the resulting unipolar bit stream to a stream of bipolar modulation symbols $\mathbf{Y}_1^R = (\mathrm{Y}_1, \mathrm{Y}_2, \ldots, \mathrm{Y}_R) = (\bar{\mathbf{y}}_1, \bar{\mathbf{y}}_2, \ldots, \bar{\mathbf{y}}_n, \ldots, \bar{\mathbf{y}}_B) = \{-1,+1\}^R$, with the length R being the number of all bits in the block, and $\bar{\mathbf{y}}_n$ being the bipolar representation of $\mathbf{y}_n$. Subsequently, transmission takes place over an additive white Gaussian noise (AWGN) channel. For hard-decision decoding (HD), the received hard-decided bipolar bit combination $\hat{\mathbf{Y}}_1^R = \{-1,+1\}^R$ is analyzed from bit position 1 to R, and the variable-length bit combinations are transformed to corresponding quantizer indices i according to a VLC decoder look-up table. In contrast, the VLC soft-decision decoder expects log-likelihood ratios (LLRs) $L(\hat{\mathbf{Y}}_1^R) = (L(\hat{\mathrm{Y}}_1), L(\hat{\mathrm{Y}}_2), \ldots, L(\hat{\mathrm{Y}}_R)) \in \mathbb{R}^R$. The LLRs representing the channel reliability information, the block length B, the bit vector length R, will be required by the VLC soft-decision decoder, in order to calculate a posteriori probabilities (APPs), and finally source symbol estimations.

2.2. Trellis Representation

In the bitstream $\mathbf{Y}_1^R$, we denote the possible positions of the last bit of $\mathbf{y}_{n-1}$ as state $s_{n-1} = \mu \in \mathcal{S}_{n-1}$, and of $\mathbf{y}_n$ as state $s_n = \nu \in \mathcal{S}_n$, respectively. Once the bit combination $\mathbf{y}_n$ of length $\nu - \mu$ is transmitted at symbol time n, the state changes from μ to ν. While the bit stream is transmitted over a noisy channel, the correct states may not be reconstructed. In order to increase the robustness of the decoder, all possible states $s_n \in \mathcal{S}_n$ at symbol time n must be considered. Utilizing the trellis representation from [24], Fig. 2 shows all possible states s_n over symbol time n. We take an example of $B = 4, R = 6$ for 2 bit quantized source symbols with the Huffman [30] codewords $\mathbf{y}^{(0)} = (1,0,1), \mathbf{y}^{(1)} = (0), \mathbf{y}^{(2)} = (1,1), \mathbf{y}^{(3)} = (1,0,0)$. Herein, $\mathbf{y}^{(i)} = (\mathrm{y}_1^{(i)}, \mathrm{y}_2^{(i)}, \cdots, \mathrm{y}_m^{(i)}, \ldots, \mathrm{y}_{N^{(i)}}^{(i)})$ denotes the codeword for the corresponding quantization codebook index i, and $\mathrm{y}_m^{(i)} \in \{0,1\}$ is the *m*th bit in $\mathbf{y}^{(i)}$. This time-varying trellis diagram reveals three distinct stages: *Diverging* (the number of states in $\mathcal{S}_n$ increases along with n), *stationary* (the number of states in $\mathcal{S}_n$ remains the same), and *converging* (the number of states decreases until reaching the known number of symbols and bits in the block (B,R)). This leads to different definitions of state boundaries in each stage. Moreover, $R - B \cdot \min(N^{(0)}, N^{(1)}, \ldots, N^{(2^M-1)}) + 1$ is the maximum number of states at a symbol time in this trellis representation, with $\min(N^{(0)}, N^{(1)}, \ldots, N^{(2^M-1)})$ being the minimum length of a codeword $\mathbf{y}^{(i)}$, $i \in \mathcal{I} = \{0,1,\ldots,2^M-1\}$.

2.3. A Posteriori Probabilities (APPs)

In the following we present the core of our VLC soft-decision decoder, having its roots in [25] and being a modification of the original BCJR algorithm [20], in a consistent fashion. According to the

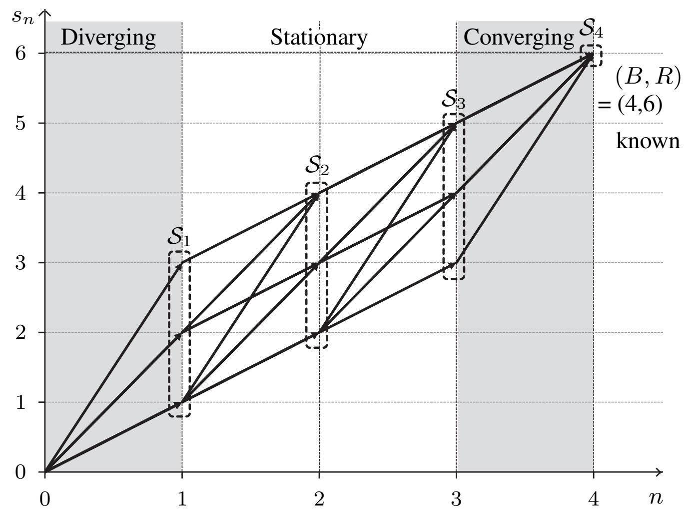

Fig. 2: Trellis representation for $B = 4, R = 6$, and the VLC being $\mathbf{y}^{(0)} = (1,0,1), \mathbf{y}^{(1)} = (0), \mathbf{y}^{(2)} = (1,1), \mathbf{y}^{(3)} = (1,0,0)$.

BCJR algorithm, the a posteriori probabilities (APPs) of a probably transmitted quantizer bit combination at symbol time n, given the received bit vector $\hat{\mathbf{Y}}_1^R$, can be written as

$$\begin{aligned} &\mathrm{P}(\mathbf{x}_n = \mathbf{x}^{(i)} | \hat{\mathbf{Y}}_1^R) = \\ &\frac{1}{C} \cdot \sum_{\mu \in \mathcal{S}_{n-1}} \sum_{\nu \in \mathcal{S}_n} \alpha_{n-1}(\mu) \cdot \gamma_n(i,\mu,\nu) \cdot \beta_n(\nu), \end{aligned} \tag{1}$$

with $\alpha_{n-1}(\mu) = p(s_{n-1} = \mu, \hat{\mathbf{Y}}_1^\mu)$ computed in the forward recursion, $\beta_n(\nu) = p(\hat{\mathbf{Y}}_{\nu+1}^R | s_n = \nu)$ computed in the backward recursion, and $\gamma_n(i,\mu,\nu) = \mathrm{P}(\hat{\mathbf{Y}}_{\mu+1}^\nu, \mathbf{x}_n = \mathbf{x}^{(i)}, s_n = \nu | s_{n-1} = \mu, \hat{\mathbf{Y}}_1^\mu)$. Herein, $\mathbf{x}_n$ at symbol time n takes on the value $\mathbf{x}^{(i)}$ being the bit combination of the quantization codebook index i. The vector of received bits from bit position a to b is denoted by $\hat{\mathbf{Y}}_a^b = (\hat{\mathrm{Y}}_a, \hat{\mathrm{Y}}_{a+1}, \ldots, \hat{\mathrm{Y}}_b) = \{-1,+1\}^{b-a+1}$. The states μ and ν are elements of the state sets $\mathcal{S}_{n-1}$ and $\mathcal{S}_n$ at previous symbol time $n-1$ and current symbol time n, respectively. The constant C normalizes the sum over the APPs to one.

2.3.1. *Forward Recursion*

The forward recursion can be processed as

$$\alpha_n(\nu) = \sum_{\mu \in \mathcal{S}_{n-1}} \sum_{i \in \mathcal{I}} \alpha_{n-1}(\mu) \cdot \gamma_n(i,\mu,\nu), \tag{2}$$

with the initial value $\alpha_0(0) = 1$, and

$$\begin{aligned} \gamma_n(i,\mu,\nu) = &\ \mathrm{P}(\hat{\mathbf{Y}}_{\mu+1}^\nu | \mathbf{x}_n = \mathbf{x}^{(i)}) \\ &\cdot \mathrm{P}(\mathbf{x}_n = \mathbf{x}^{(i)}, s_n = \nu | s_{n-1} = \mu, \hat{\mathbf{Y}}_1^\mu), \end{aligned} \tag{3}$$

which consists of a *channel term* and a *source probability distribution term*.

Assuming a memoryless channel, the probability of the received vector $\hat{\mathbf{Y}}_{\mu+1}^\nu$, given a possibly transmitted quantizer bit combination, are determined by the *channel term* [13]

$$\mathrm{P}(\hat{\mathbf{Y}}_{\mu+1}^{\nu}|\mathbf{x}_n=\mathbf{x}^{(i)}) = \mathrm{P}(\hat{\mathbf{Y}}_{\mu+1}^{\nu}|\mathbf{y}_n=\mathbf{y}^{(i)}) = \prod_{m=1}^{N^{(i)}} \mathrm{P}(\hat{\mathrm{Y}}_{\mu+m}|\mathrm{y}_m^{(i)}). \tag{4}$$

Herein, $\hat{\mathrm{Y}}_{\mu+m}$ denotes the received hard-decided bit at bit position $\mu+m$. The conditional *bit* probability is formulated as

$$\mathrm{P}(\hat{\mathrm{Y}}_{\mu+m}|\mathrm{y}_m^{(i)}) = \begin{cases} 1-\mathrm{BER}_m, & \text{if } \hat{\mathrm{Y}}_{\mu+m} = \bar{\mathrm{y}}_m^{(i)}, \\ \mathrm{BER}_m, & \text{else,} \end{cases} \tag{5}$$

with the bit error probability $\mathrm{BER}_m = \frac{1}{1+\exp(|L(\hat{\mathrm{Y}}_{\mu+m})|)}$, and $\bar{\mathrm{y}}_m^{(i)}$ being the *m*th bit of codeword $\mathbf{y}^{(i)}$ in bipolar notation. The LLRs can be acquired by $L(\hat{\mathrm{Y}}_{\mu+m}) = 4 \cdot \frac{E_b}{N_0} \cdot \tilde{\mathrm{Y}}_{\mu+m}$, with E_b being the signal energy per bit, N_0 being the noise power spectral density, and $\tilde{\mathrm{Y}}_{\mu+m}$ being the real-valued signal observed at the (noisy) transmission channel output (note that $\hat{\mathrm{Y}}_{\mu+m} = \mathrm{sign}(\tilde{\mathrm{Y}}_{\mu+m})$).

The quantized parameters can be modeled as zeroth-order Markov process resulting in zeroth-order a priori knowledge (AK0), or as first-order Markov process, leading to first-order a priori knowledge (AK1). The AK0 and AK1 are obtained by counting the occurence frequency for different pairs of quantizer output symbols from a large training database [13]. Thereafter, according to the chain rule, an AK1 term is calculated by

$$\mathrm{P}(\mathbf{x}_n=\mathbf{x}^{(i)}|\mathbf{x}_{n-1}=\mathbf{x}^{(j)}) = \frac{\mathrm{P}(\mathbf{x}_n=\mathbf{x}^{(i)}, \mathbf{x}_{n-1}=\mathbf{x}^{(j)})}{\sum_{k\in\mathcal{I}} \mathrm{P}(\mathbf{x}_n=\mathbf{x}^{(k)}, \mathbf{x}_{n-1}=\mathbf{x}^{(j)})}, \tag{6}$$

and an AK0 term $\mathrm{P}(\mathbf{x}_n = \mathbf{x}^{(i)})$ is obtained by marginalization of the numerator in (6).

Taking source correlation into account, the *source probability distribution term* in (3) can be written as

$$\begin{aligned} &\mathrm{P}(\mathbf{x}_n = \mathbf{x}^{(i)}, s_n = \nu | s_{n-1} = \mu, \hat{\mathbf{Y}}_1^{\mu}) = \\ &\sum_{j\in\mathcal{I}} \mathrm{P}(\mathbf{x}_n = \mathbf{x}^{(i)}, s_n = \nu | \mathbf{x}_{n-1} = \mathbf{x}^{(j)}, s_{n-1} = \mu) \\ &\cdot \mathrm{P}(\mathbf{x}_{n-1} = \mathbf{x}^{(j)} | s_{n-1} = \mu, \hat{\mathbf{Y}}_1^{\mu}). \end{aligned} \tag{7}$$

According to AK1, the first term on the right-hand-side of (7) can be computed as follows:

$$\begin{aligned} &\mathrm{P}(\mathbf{x}_n = \mathbf{x}^{(i)}, s_n = \nu | \mathbf{x}_{n-1} = \mathbf{x}^{(j)}, s_{n-1} = \mu) = \\ &\frac{1}{C_1(\mu, j)} \cdot \begin{cases} \mathrm{P}(\mathbf{x}_n = \mathbf{x}^{(i)} | \mathbf{x}_{n-1} = \mathbf{x}^{(j)}), & \text{if } \nu - \mu = N^{(i)}, \\ 0, & \text{else,} \end{cases} \end{aligned} \tag{8}$$

with the normalization

$$C_1(\mu, j) = \sum_{\nu' \in \mathcal{S}_n} \sum_{i\in\mathcal{I}: N^{(i)} = \nu' - \mu} \mathrm{P}(\mathbf{x}_n = \mathbf{x}^{(i)} | \mathbf{x}_{n-1} = \mathbf{x}^{(j)}). \tag{9}$$

Considering the last bit position $\lambda = \mu - N^{(j)}$ of $\mathbf{x}_{n-2}$ [25], the latter term on the right-hand-side of (7) can be expressed as

$$\mathrm{P}(\mathbf{x}_{n-1} = \mathbf{x}^{(j)} | s_{n-1} = \mu, \hat{\mathbf{Y}}_1^{\mu}) = \frac{1}{C_2(\mu)} \alpha_{n-2}(\lambda) \cdot \gamma_{n-1}(j, \lambda, \mu), \tag{10}$$

with

$$C_2(\mu) = \sum_{j' \in \mathcal{I}} \alpha_{n-2}(\lambda = \mu - N^{(j')}) \cdot \gamma_{n-1}(j', \lambda = \mu - N^{(j')}, \mu). \tag{11}$$

It can be seen that $\lambda = \mu - N^{(j)}$ is uniquely determined by μ and the codeword length of index j, and each C_2 value corresponds to one state μ. Moreover, the terms $\alpha_{n-2}(\lambda)$ and $\gamma_{n-1}(j, \lambda, \mu)$ will be zero if $\lambda \notin \mathcal{S}_{n-2}$.

If AK0 is adopted, the latter term of the right-hand-side of (3) changes to

$$\begin{aligned} &\mathrm{P}(\mathbf{x}_n = \mathbf{x}^{(i)}, s_n = \nu | s_{n-1} = \mu, \hat{\mathbf{Y}}_1^{\mu}) = \\ &\frac{1}{C_1'(\mu)} \cdot \begin{cases} \mathrm{P}(\mathbf{x}_n = \mathbf{x}^{(i)}), & \text{if } \nu - \mu = N^{(i)}, \\ 0, & \text{else,} \end{cases} \end{aligned} \tag{12}$$

with the normalization (equal to one in the diverging stage)

$$C_1'(\mu) = \sum_{\nu' \in \mathcal{S}_n} \sum_{i\in\mathcal{I}: N^{(i)} = \nu' - \mu} \mathrm{P}(\mathbf{x}_n = \mathbf{x}^{(i)}). \tag{13}$$

Note that not all transitions from $s_{n-1} = \mu$ to $s_n = \mu + N^{(i)}$, with i from 0 to $2^M - 1$, are available both in the stationary and the converging stage of the VLC trellis representation (Fig. 2) in formulae (9) and (13) (i.e., $C_1(\mu, j)$ and $C_1'(\mu)$ are not always equal to one).

2.3.2. Backward Recursion

The backward recursion can be computed as

$$\beta_n(\nu) = \sum_{\omega \in \mathcal{S}_{n+1}} \sum_{h \in \mathcal{I}} \gamma_{n+1}'(h, \nu, \omega) \cdot \beta_{n+1}(\omega), \tag{14}$$

with the initial value of β being $\beta_B(R) = 1$, and

$$\begin{aligned} \gamma_{n+1}'(h, \nu, \omega) &= \mathrm{P}(\hat{\mathbf{Y}}_{\nu+1}^{\omega} | \mathbf{x}_{n+1} = \mathbf{x}^{(h)}) \\ &\cdot \mathrm{P}(\mathbf{x}_{n+1} = \mathbf{x}^{(h)}, s_{n+1} = \omega | s_n = \nu). \end{aligned} \tag{15}$$

The states ν and ω are elements of state sets $\mathcal{S}_n$ and $\mathcal{S}_{n+1}$ at the current symbol time n and next symbol time $n+1$, respectively.

The *channel term* is given in analogy to (4) and (5) as

$$\mathrm{P}(\hat{\mathbf{Y}}_{\nu+1}^{\omega} | \mathbf{x}_{n+1} = \mathbf{x}^{(h)}) = \prod_{m=1}^{N^{(h)}} \mathrm{P}(\hat{\mathrm{Y}}_{\nu+m} | \mathrm{y}_m^{(h)}). \tag{16}$$

The *source probability distribution term* is obtained by

$$\begin{aligned} &\mathrm{P}(\mathbf{x}_{n+1} = \mathbf{x}^{(h)}, s_{n+1} = \omega | s_n = \nu) = \\ &\frac{1}{C_3(\nu)} \cdot \begin{cases} \mathrm{P}(\mathbf{x}_{n+1} = \mathbf{x}^{(h)}), & \text{if } \omega - \nu = N^{(h)}, \\ 0, & \text{else,} \end{cases} \end{aligned} \tag{17}$$

with the normalization taking the special case of stationary and converging stages into account again:

$$C_3(\nu) = \sum_{\omega' \in \mathcal{S}_{n+1}} \sum_{h\in\mathcal{I}: N^{(h)} = \omega' - \nu} \mathrm{P}(\mathbf{x}_{n+1} = \mathbf{x}^{(h)}). \tag{18}$$

2.4. Source Symbol Estimation

Using the APPs (1) and the quantizer codebook, the source symbol u_n can now be estimated. As minimum mean-square error (MMSE) estimation maximizes the value of the signal-to-noise ratio (SNR), it is adopted in the following and the global SNR is used to evaluate the performance:

$$\hat{u}_n = \sum_{i\in\mathcal{I}} u^{(i)} \cdot \mathrm{P}(\mathbf{x}_n = \mathbf{x}^{(i)} | \hat{\mathbf{Y}}_1^R), \tag{19}$$

with $u^{(i)}$ being the entry of the quantization codebook corresponding to index i.

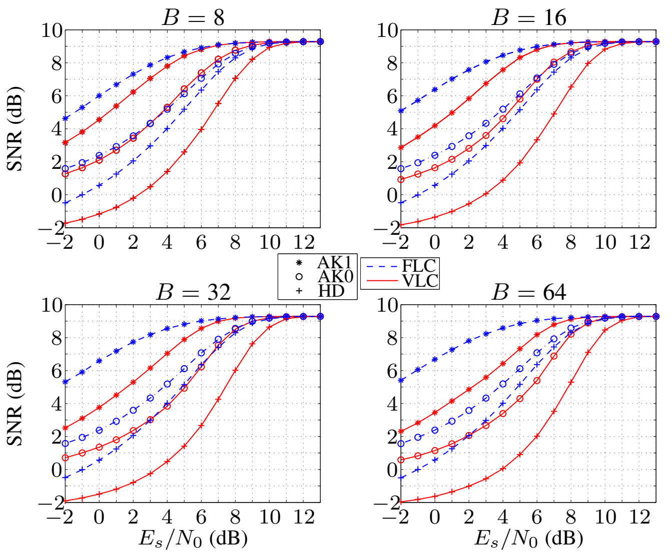

Fig. 3: Simulation results for an $M = 2$ bit quantized Gaussian AR(1) process with different block lengths B.

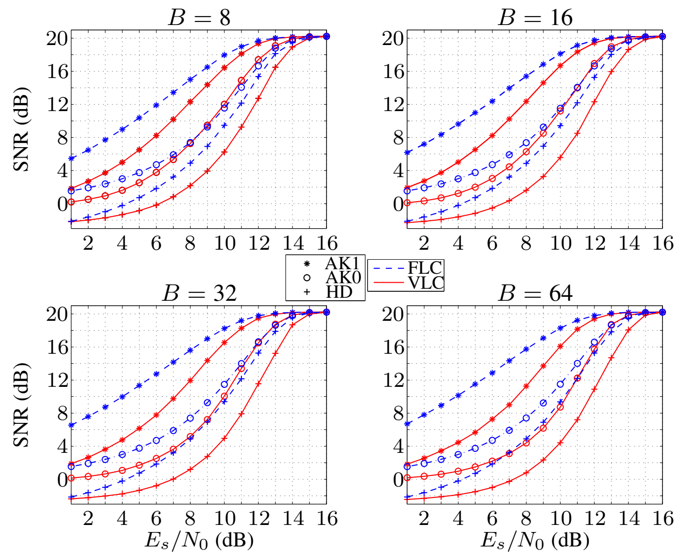

Fig. 4: Simulation results for an $M = 4$ bit quantized Gaussian AR(1) process with different block lengths B.

3. SIMULATIONS

3.1. Simulation Setup

The highly correlated samples of a first order autoregressive (AR(1)) Gaussian process with zero mean, unit variance, and correlation coefficient being 0.9 are used as source symbols. Loyd-Max quantizers with 2 bit and 4 bit are utilized in two separate simulations (Fig. 3 and Fig. 4, respectively). The quantizer bit combinations are obtained according to the natural binary code (NBC) [31]. For both simulations, a number of 10^8 source symbols is utilized as the training database to obtain AK1 and AK0 according to (6). Besides, in each simulation, a number of 640000 fixed source symbols are divided into block lengths of either 8, 16, 32, or 64, respectively. Moreover, each block is transmitted over different channel realizations for a given E_b/N_0. Finally, the performance is evaluated according to the global SNR of these 640000 source symbols. To solve numerical issues in good channel conditions, all terms in the above formulae are implemented in the log domain; the APPs are transformed to the linear domain just before source symbol estimation (19).

As VLCs and FLCs have different bit rates, a fair comparison between VLC and FLC soft-decision decoding requires the energy per source symbol E_s being the same in all simulations[1]. According to $\mathrm{P}(\mathbf{x}^{(i)})$ (AK0), the variable-length codes are generated by standard Huffman coding resulting in two separate Huffman codebooks for $M \in \{2, 4\}$ bit. Two algorithms are compared: The variable-length soft-decision decoding (VLC/SD) according to Section 2, and fixed-length soft-decision decoding (FLC/SD) with APPs from the original BCJR algorithm [20].

3.2. Discussion

In Figs. 3 and 4, HD denotes hard-decision decoding, AK0 and AK1 represent soft-decision decoding (SD) with zeroth-order and first-order a priori knowledge, respectively. As can be seen in both figures, the use of AK0 (no source correlation (used), but histogram-related residual redundancy) leads to obvious improvements versus HD in all cases. Clear further improvements are obtained when using AK1 (source correlation used in addition) — both for VLCs and FLCs. As shown from [13], all SD results show a minimum of SNR = 0 dB at worst channel conditions.

Varying the block length, we observe that for both HD and AK0, the performance for FLC decoders remains constant, while the VLC decoders loose performance for longer block lengths. For medium to good channel qualities and short block lengths ($B \leq 16$), however, the VLC/AK0 scheme even outperforms the FLC/AK0 approach (compare to [17]). Since using AK0 is equivalent to using AK1 in the case of uncorrelated source symbols, we can state that, in these conditions, VLC may be a better choice than FLC for uncorrelated sources on AWGN channels — but only if soft-decision decoding is employed. This effect is even more prominent for the lower bit rate ($M = 2$ bit). Using the AK1 scheme for correlated source symbols, it turns out that FLC/SD is by far more powerful than VLC/SD — for both quantizers and all block lengths. Moreover, FLC/AK1 shows increased performance for longer block lengths due to a reduced influence of initialization. In contrast, the performance of VLC/AK1 decreases again for longer block lengths.

4. CONCLUSIONS

In this paper we have presented a variable-length (VLC) soft-decision (SD) decoder. It is able to utilize residual redundancy in the source symbols. Simulations over an AWGN channel showed that certain degrees of residual redundancy allow for significant improvements. Compared to fixed-length (FLC) soft-decision decoding, the VLC/SD approach exceeds the FLC/SD approach for uncorrelated sources and short block lengths with medium to good channel qualities. For correlated sources, FLC/SD turns out to be the best scheme in all simulated conditions.

[1] This means for the 2 bit quantizer $2 * E_b^{\mathrm{FLC}} = E_s = 1.9896 * E_b^{\mathrm{VLC}}$, and the 4 bit quantizer $4 * E_b^{\mathrm{FLC}} = E_s = 3.8093 * E_b^{\mathrm{VLC}}$, given the average Huffman codeword length of the respective VLC.

5. REFERENCES

[1] "Digital Cellular Telecommunications System: Substitution and Muting of Lost Frames for Enhanced Full Rate (EFR) Speech Traffic Channels (GSM 06.61)," ETSI TC-SMG, Feb. 1996.

[2] "Mandatory Speech Codec Speech Processing Functions: AMR Speech Codec; Error Concealment of Lost Frames (3GPP TS 26.091)," 3GPP; TSG-SA, Dec. 1999.

[3] "Adaptive Multi-Rate - Wideband (AMR-WB) Speech Codec; Error Concealment of Erroneous or Lost Frames; (3GPP TS 26.191)," 3GPP; TSG-SA, Mar. 2001.

[4] J. Hagenauer and P. Hoeher, "A Viterbi Algorithm with Soft-Decision Outputs and its Applications," in *Proc. of GLOBE-COM*, Dallas, TX, USA, Nov. 1989, pp. 1680–1686.

[5] J. Huber and A. Rüppel, "Zuverlässigkeitsschätzung für die Ausgangssymbole von Trellis-Decodern," *AEÜ* (in German), vol. 44, no. 1, pp. 8–21, Jan. 1990.

[6] V. Cuperman, F.-H. Liu, and P. Ho, "Robust Vector Quantization for Noisy Channels Using Soft Decision and Sequential Decoding," *Europ. Trans. Telecomm.*, vol. 5, no. 5, pp. 7–18, Sept. 1994.

[7] N. Farvardin and V. Vaishampayan, "Optimal Quantizer Design for Noisy Channels: An Approach to Combined Source-Channel Coding," *IEEE Trans. Inf. Theory*, vol. 33, no. 6, pp. 827–838, Nov. 1987.

[8] F. Liu, P. Ho, and V. Cuperman, "Sequential Reconstruction of Vector Quantized Signals Transmitted over Rayleigh Fading Channels," in *Proc. of IEEE International Conference on Communications*, New Orleans, LA, USA, May 1994, vol. 1, pp. 23–27.

[9] M. Skoglund and P. Hedelin, "Vector Quantization Over a Noisy Channel Using Soft Decision Decoding," in *Proc. of ICASSP 94*, Adelaide, Australia, Apr. 1994, vol. 5, pp. 605–608.

[10] T. Fingscheidt, P. Vary, and J.A. Andonegui, "Robust Speech Decoding: Can Error Concealment be Better Than Error Correction?," in *Proc. of ICASSP 1998*, Seattle, WA, USA, May 1998, vol. 1, pp. 373–376.

[11] T. Fingscheidt, "Parameter Models and Estimators in Soft Decision Source Decoding," in *Advances in Digital Speech Transmission*, R. Martin, U. Heute, and C. Antweiler, Eds., pp. 281–310. John Wiley & Sons, Ltd, West Sussex, England, 2008.

[12] T. Fingscheidt, "Graceful Degradation in ADPCM Speech Transmission," in *Proc. of DAGA*, Aachen, Germany, Mar. 2003, pp. 748–749.

[13] T. Fingscheidt and P. Vary, "Softbit Speech Decoding: A New Approach to Error Concealment," *IEEE Trans. Speech, Audio Process.*, vol. 9, no. 3, pp. 240–251, Mar. 2001.

[14] F. Pflug and T. Fingscheidt, "Delayless Soft-Decision Decoding of High-Quality Audio Transmitted Over AWGN Channels," in *Proc. of ICASSP 2011*, Prague, Czech Republic, May 2011, pp. 489–492.

[15] S. Han, F. Pflug, and T. Fingscheidt, "Improved AMR Wideband Error Concealment for Mobile Communications," in *Proc. of EUSIPCO 2013*, Marrakech, Morocco, Sept. 2013.

[16] J. Wen and J.D. Villasenor, "Utilizing Soft Information in Decoding of Variable Length Codes," in *Proc. of Data Compression Conference*, Snowbird, UT, USA, Mar. 1999, pp. 131–139.

[17] M. Park and D.J. Miller, "Joint Source-Channel Decoding for Variable-Length Encoded Data by Exact and Approximate MAP Sequence Estimation," *IEEE Trans. Commun.*, vol. 48, no. 1, pp. 1–6, 2000.

[18] N. Demir and K. Sayood, "Joint Source/Channel Coding for Variable Length Codes," in *Proc. of Data Compression Conference*, Snowbird, UT, USA, Mar. 1998, pp. 139–148.

[19] A.H. Murad and T.E. Fuja, "Joint Source-channel Decoding of Variable-Length Encoded Sources," in *Proc. of Information Theory Workshop*, Killarney, Ireland, June 1998, pp. 94–95.

[20] L.R. Bahl, J. Cocke, F. Jelinek, and J. Raviv, "Optimal Decoding of Linear Codes for Minimizing Symbol Error Rate," *IEEE Trans. Inf. Theory*, vol. 20, pp. 284–287, Mar. 1974.

[21] R. Bauer and J. Hagenauer, "On Variable Length Codes for Iterative Source/Channel Decoding," in *Proc. of Data Compression Conference*, Snowbird, UT, USA, Mar. 2001, pp. 273–282.

[22] R. Thobaben and J. Kliewer, "Low-Complexity Iterative Joint Source-Channel Decoding for Variable-Length Encoded Markov Sources," *IEEE Trans. Commun.*, vol. 53, no. 12, pp. 2054–2064, 2005.

[23] V.B. Balakirsky, "Joint Source-Channel Coding with Variable Length Codes," in *Proc. of IEEE International Symposium on Information Theory*, Ulm, Germany, June 1997, p. 419.

[24] B. Rainer and J. Hagenauer, "Symbol-by-Symbol MAP Decoding of Variable Length Codes," in *Proc. of 3rd ITG Conference "Source and Channel Coding"*, Munich, Germany, Jan. 2000, pp. 111–116, VDE–Verlag.

[25] J. Kliewer and R. Thobaben, "Iterative Joint Source-Channel Decoding of Variable-Length Codes Using Residual Source Redundancy," *IEEE Trans. Wireless Commun.*, vol. 4, no. 3, pp. 919–929, 2005.

[26] W. Xiang, S.S. Pietrobon, and S.A. Barbulescu, "Iterative Decoding of JPEG Coded Images with Channel Coding," in *Proc. of International Conference on Telecommunications*, Anchorage, AK, USA, May 2003, vol. 2, pp. 1356–1360.

[27] C. Bergeron and C. Lamy-Bergot, "Soft-Input Decoding of Variable-Length Codes Applied to the H.264 Standard," in *Proc. of IEEE Workshop on Multimedia Signal Processing*, Siena, Italy, Sept. 2004, pp. 87–90.

[28] C.M. Lee, M. Kieffer, and P. Duhamel, "Soft Decoding of VLC Encoded Data for Robust Transmission of Packetized Video," in *Proc. of ICASSP 2005*, Philadelphia, PA, USA, Mar. 2005, vol. 3, pp. iii/737–iii/740.

[29] O. Derrien, M. Kieffer, and P. Duhamel, "Joint Source/Channel Decoding of Scalefactors in MPEG-AAC Encoded Bitstreams," in *Proc. of EUSIPCO 2008*, Lausanne, Switzerland, Aug. 2008.

[30] D.A. Huffman, "A Method for the Construction of Minimum-Redundancy Codes," *Proceedings IRE*, vol. 40, no. 9, pp. 1098–1101, Sept. 1952.

[31] N.S. Jayant and P. Noll, *Digital Coding of Waveforms*, Prentice-Hall, Inc., Englewood Cliffs, New Jersey, 1984.